Anisotropy in the Raman scattering of a CaFeO<inf>2.5</inf> single crystal and its link with oxygen ordering in Brownmillerite frameworks

Andrea Piovano, Monica Ceretti, Mark Johnson, Giovanni Agostini, Werner Paulus, Carlo Lamberti

"Anisotropy in the Raman scattering of a $CaFeO_{2.5}$ single crystal and its link with oxygen ordering in Brownmillerite frameworks"

J. Phys.: Condensed Matter, **27** *(2015)* Art. n. 225403. (11 pages).

doi:10.1088/0953-8984/27/22/225403

Anisotropy in the Raman scattering of a $CaFeO_{2.5}$ single crystal and its link with oxygen ordering in Brownmillerite frameworks

Andrea Piovano[1,*], Monica Ceretti[2], Mark Johnson[1], Giovanni Agostini[3], Werner Paulus[2], Carlo Lamberti[4,5]

[1] *Institut Laue-Langevin (ILL), BP 156 X, F-38042 Grenoble Cedex, France*
[2] *University of Montpellier 2, UMR 5253, ICGM, C2M, CC1504, 5 Place Eugène Batallion, 34095 Montpellier, France*
[3] *European Synchrotron Radiation Facility (ESRF) 6 Rue Jules Horowitz, BP 220 38043 Grenoble Cedex, France*
[4] *Department of Chemistry, NIS Center of Excellence, CrisDi center for crystallography and INSTM unit, University of Turin, Via Giuria 7, I-10125, Turin, Italy*
[5] *Southern Federal University, Zorge street 5, 344090 Rostov-on-Don, Russia*

Abstract. Periodic DFT calculations allow understanding the strong orientation dependent Raman spectra of oriented $CaFeO_{2.5}$ single crystals. Modes involving the oscillation of the apical oxygen (O_{ap}) atoms were found to be strongly enhanced when the electric field of the linearly polarized laser line is parallel to *b*. For $CaFeO_{2.5}$ ordered system strong polarizability of these modes go along with strong Raman intensities. Conversely, the apical oxygen disorder observed in oxygen conduction $SrFeO_{2.5}$ destroys the long range coherence of the respective Raman modes, which consequently show a strongly reduced intensity. This study provides a vibrational tool to discriminate between ordered and disordered isomorporphous $ABO_{2.5}$ Brownmillerite frameworks. Furthermore, in combination with DFT calculations, we found that the weakening of the interlayer interactions is responsible for the loss of ordering in some of the Brownillerite compounds.

1. Introduction

The search of oxygen ion conductors already operating at moderate temperature is attracting considerable interest as they have potential technological applications in devices such as Solid Oxide Fuel Cells (SOFC) [1-14]. Materials that are presently in use work at high (900-1000 °C) or intermediate (500-750 °C) [10] temperatures with consequent problems of chemical and mechanical stability with time [9]. In this regard, promising materials are oxides with Brownmillerite type structure, which are oxygen deficient perovskites with an overall stoichiometry of $ABO_{2.5}$, showing in some case oxygen mobility down to ambient temperature [15-17].

The Brownmillerite framework is an oxygen vacancy ordered framework, consisting of alternating octahedral BO_6 and tetrahedral BO_4 layers. Each $(BO_4)_\infty$ tetrahedra chain bridging can principally point into two directions referred to L and R, while the space group symmetry of the brownmillerite framework depends on the symmetry relation between L and R chains [15, 18-22]. Within the orthorhombic unit cell, random distribution of all L and R chains results in a special disorder scenario of the $(BO_4)_\infty$ chains which can be described in the *Imma* space group, implying a split position of the tetrahedral B cations and associated tetrahedral in-plane oxygen atoms. Brownmillerite frameworks showing an ordered $(BO_4)_\infty$ chains arrangement are generally described in the *I2mb* space group, with all tetrahedra pointing toward the same direction (only L or R chains are present), or in the *Pnma* space group, with ordered alternation of L and R chains along the *b* axis is present.

Symmetry operations of the transformation of the L chain into the R one and vice versa are also symmetry operations of the underlying perovskite structure, which should lead in principle to the same configurational energy for the two sets [19-26]. The L↔R transformation does not change the first coordination spheres of the A and B cations and does not noticeably alter the interatomic distances.[17] Nevertheless, for different combinations of A and B cations different tetrahedra ordering schemes were found experimentally [15, 17, 19, 27].

With their studies Kruger et al. [24, 25] showed that the thermal expansion of the $CaFeO_{2.5}$ structure, the distances between the tetrahedral layers increase disproportionally more compared with the rest of the structure. With increasing distance between the tetrahedral layers, they suppose it becomes energetically more reasonable to compensate the dipole moments within the layers. The aperiodic order of the sequence of tetrahedral chains can be assumed to minimize the structural distortions, which would be induced by a strictly alternating sequence. Moreover they argued that anti-phase boundaries (APBs) can form if different domains of the *Pnma* structure grow and contact together, producing thin slabs of *I2mb* structure within the *Pnma* matrix.

On their side, Auckett et al. [28] studied the behavior of long-range chain ordering in $Sr_2Fe_2O_5$. They found that the apical oxygen atoms are more mobile than those at other positions and display anisotropic motion in the direction of the tetrahedral layer. Their electron diffraction patterns suggest that such ordered sequences are present at least locally, and the diffuse intensity lines on these patterns arise from the areas where long-range order between the layers is absent.

These findings had been confirmed by the TEM work by D'Hondt et al. [20] where the diffuse intensity lines on the ED patterns demonstrate that disorder is also present in the stacking sequence of the tetrahedral layers. The transmission electron microscopy investigation clearly revealed that the L and R tetrahedral chains in the $Sr_2Fe_2O_5$ structure form perfect two-dimensional order within the tetrahedral layers according to the -L-R-L-R-sequence. Such an arrangement of the tetrahedral chains within the layer looks most favorable for the mutual compensation of the opposite dipoles associated with the L and R chains because it provides the shortest separation between the chains of different types. In contrast to that, no significant energy gain is related to the ordering of the tetrahedral layers because changing the stacking sequence by a mutual displacement of the layers does not alter the nearest-neighbor separations between the L and R chains. In definitive this causes the simultaneous presence of areas with different ordered stacking sequences of the layers and local areas of disordered stacking.

Abakumov et al. [18] have proposed a model which implies that a significant part of the tetrahedral chains can change their rotation sense so that an L-chain becomes an R-chain and vice versa to explain the findings obtained on a Sr_2MnGaO_5 brownmillerite. The transformation of chains of different types into each other may occur at point defects such as oxygen vacancies or the presence of a cation with a different coordination, e.g. a square planar coordination. They suggested as possible driving factors the size of the A and B cations and the electronic configuration of the B cation.

In spite of numerous structural data available on Brownmillerite compounds and the numerous assumptions on the origin of the different structural arrangements, there is not yet a clear evidence of what is the driving force causing tetrahedral chain ordering, when present. Few can be said without using a spectroscopic technique.

To clarify if the origin of the ordering or disordering of the Brownmillerite structures is connected to the presence or not of specific modification of intralayer or interlayer interactions, a technique that permits to gather information on the electron configuration and at the vibrational behavior of the materials is necessary. Raman spectroscopy is the most promising one, as it can look at both properties at the same time. The analysis of the homologous $CaFeO_{2.5}$ and $SrFeO_{2.5}$ systems, the former crystallizing in the ordered *Pnma* structure, the latter showing a disordered arrangement of thetrahedra that can be indexed in the average *Imma* space group, should permit to a better understanding on the ordering driving forces.

Here we present an orientation dependent Raman analysis of oriented $CaFeO_{2.5}$ single crystals, together with Raman spectra of isostructural Brownmillerite powders and related simulations. The single crystal analysis highlighted the anisotropy of optical response of this system and parallel DFT calculation helped understanding how the electronic configuration is connected to this behavior. The comparison between the Raman spectra collected on (ordered) $CaFeO_{2.5}$ and (disordered) $SrFeO_{2.5}$ powders, allowed us to understand that changes in the lattice dynamics involving the apical oxygen atoms that could be used to discriminate between ordered or disordered behavior. Ab-initio methods are in this context the most promising tool for computational studies of the vibrational and electronic behavior of complex material as mixed valence oxides [16, 29-34].

2. Experimental and methods

2.1. Samples

Polycrystalline $CaFeO_{2.5}$ was prepared by intimate mixing, in presence of acetone, of high purity $CaCO_3$ (99.95%, Aldrich) and Fe_2O_3 (99.99%, Aldrich) in stoichiometric proportions. Once dried, the mixture was calcined in air at 1273 K for 24 hours three times in order to reach the desired stoichiometry resulting in a dark reddish color. The single-crystal $CaFeO_{2.5}$ was synthesized from polycrystalline sample of $CaFeO_{2.5}$, using a NEC (SC2) image furnace equipped with two 500 W halogen lamps and two optical mirrors. For a detailed explanation of the method see ref. [27]. The crystalline quality and precise orientation of the $CaFeO_{2.5}$ single crystal has been previously determined by neutron diffraction on the 5C2 single crystal diffractometer at the ORPHEE reactor (LLB Saclay, F) [27].

Polycrystalline $SrFeO_{2.5}$ was obtained starting from a mixture of stoichiometric amounts of $SrCO_3$ (99.9%, Aldrich) and Fe_2O_3 (99.99%, Aldrich). The mixture was calcined in air at 1273 K for 24 hours and afterwards ground and pressed in 1 g weight and 13mm diameter pellets. It is well known that the oxygen stoichiometry in the $SrFeO_{2.5+x}$ compound is strongly dependent on

the temperature and oxygen partial pressure. Therefore, a great effort was performed in order to precisely control oxygen content and crystalline quality of $SrFeO_{2.5}$ sample. The best preparation found consisted in heating at 1273 K in air for 24 hours followed by a further annealing in air at 1473 K for another 24 hours. Finally, to reach the exact stoichiometry, the pellets were again annealed at 1273 K and then slowly cooled under vacuum. This method allowed an important reduction of the presence of stacking faults in the structure along the *b* axis.

2.2. Raman scattering

Raman measurements on the oriented single crystal of $CaFeO_{2.5}$ and polycrystalline powders have been performed using an InVia Renishaw Raman Microscope in backscattering geometry, equipped with a 785 nm linearly polarized laser line (z direction of incoming beam in our reference system) profiting the linearly polarized light (along y-direction). Polarization analyzer was not present in our configuration. Nevertheless in our InVia spectrometer, the detection line is polarized 80% along y-direction by the diffracting grating. This z(y 80%y)-z configuration should allow all vibrational modes with enough Raman intensity, but enhance A_g modes respect to B_g modes. The availability of an oriented single crystal, mounted on a home-made rotating stage with a precision of $\pm 0.5^{\circ}$, allows perturbing the electron configuration along the direction of the electric field (***E***) of the linearly polarized laser. After several preparatory tests with the different excitations lasers present in our laboratory (wavelengths 785, 514, 442, 325, 244 nm), [35-37] the chosen laser wavelength was 785 nm. This because for first-order Raman measurements we would avoid any resonance effect due to direct transitions to real electronic states (see also Figure 1a, where the UV-Vis spectrum of polycrystalline $CaFeO_{2.5}$ is reported superimposed with the available laser lines). Finally the maximum power used was 1% of the total laser power of about 100 mW to avoid radiation damage problems. The spectra reported here were obtained averaging 5 subsequent spectra each of them collected with an integration time of 20 s cm^{-1}. Acquisition parameters were kept all fixed along the experiment to allow direct comparison among the spectra collected with different sample configurations.

2.3. Computational details

DFT calculations have been performed using the VASP code [38]. Calculations were performed in the frame of density functional theory using plane waves basis set and PAW type pseudopotential and PBE functional with a total number of 43419 plane-waves. 6, 8, 8 valence electron are calculated for O, Ca and Fe, respectively. For the one electron properties the crystallographic cell was employed with a final mesh of 8 x 4 x 8 in reciprocal space, while for computing the vibrational behavior it was employed a 1x1x1 net in reciprocal space from a supercell 2 x 1 x 2 of about 14 Å side, to take in account for long range Coulomb interactions. Raman frequencies results systematically underestimated at the PBE level of theory due to the lack of exact exchange part. In order to compare with experiment a scaling factor 1.07 has been obtained by fitting procedure in accordance with previous works [39, 40].

3. Results and discussion

The structure of $CaFeO_{2.5}$ is orthorhombic with *Pnma* space group and associated lattice parameters a = 5.430(2) Å, b = 14.76(2) Å and c = 5.601(4) Å. It belongs to the general point group D_{2h} (mmm).[41] From a structural point of view $CaFeO_{2.5}$ shows three atoms residing in the 8d Wyckoff position, two in the 4c one and only one in the 4a, [27] and the decomposition of the mechanical representation in irreducible representations is:

$$\Gamma = 13\ A_g + 14\ A_u + 11\ B_{1g} + 16\ B_{1u} + 13\ B_{2g} + 14 B_{2u} + 11\ B_{3g} + 16\ B_{3u}$$

The structure of $CaFeO_{2.5}$ comprises 105 vibrational modes, after removal of the 3 translations, which can be classified as follows: (i) 48 only Raman active; (ii) 43 only IR active; (iii) 14 IR and Raman silent. The Fe atom in the 4a Wyckoff position, i.e. in octahedral coordination, does not move for any Raman active mode.

The Raman activity is connected with the electric field of the excitation light by the polarizability tensor by the relation $\mathbf{p} = \boldsymbol{\alpha}\mathbf{E}$, where $\boldsymbol{\alpha}$ that can be decomposed respect to the point symmetry as follows:

$$\alpha_{Ag} = \begin{pmatrix} a & 0 & 0 \\ 0 & b & 0 \\ 0 & 0 & c \end{pmatrix}; \qquad \alpha_{B1g} = \begin{pmatrix} 0 & d & 0 \\ d & 0 & 0 \\ 0 & 0 & 0 \end{pmatrix};$$

$$\alpha_{B2g} = \begin{pmatrix} 0 & 0 & e \\ 0 & 0 & 0 \\ e & 0 & 0 \end{pmatrix}; \qquad \alpha_{B3g} = \begin{pmatrix} 0 & 0 & 0 \\ 0 & 0 & f \\ 0 & f & 0 \end{pmatrix}.$$

It is then clear than in a Raman experiment with z(y 80%y)-z scattering geometry, it is possible to selectively favor the α_{Ag} component and, in it, the *a*, *b* or *c* component by opportunely rotating a single crystal respect to the spectrometer axes. Whether a Raman-active phonon can be observed under certain experimental conditions regarding the incoming and scattered polarisation or not is determined by $I \propto |e_i\ \alpha\ e_s|^2$.

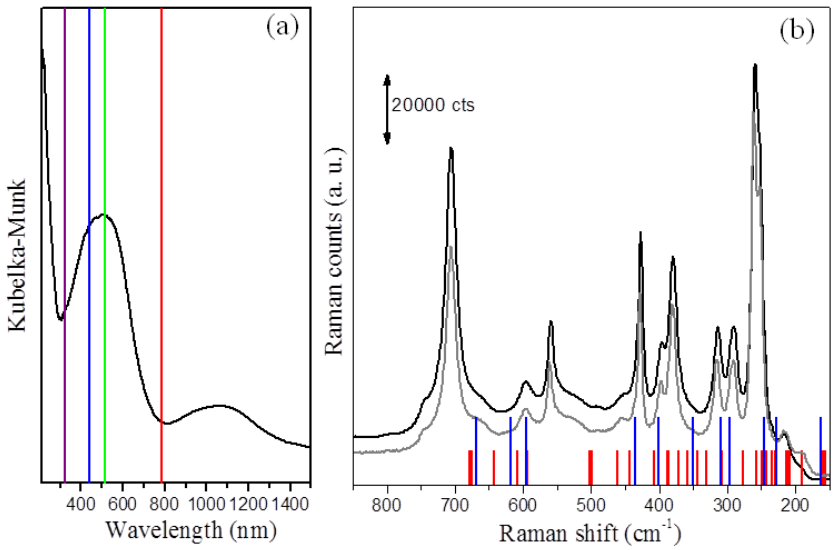

Figure 1. (a) UV-vis diffuse reflectance spectrum of $CaFeO_{2.5}$ system with superimposed the different laser lines tested; (b) Raman spectra in the z(y 80%y)-z scattering configuration of powdered $CaFeO_{2.5}$ from ground single crystal (black curve) and $CaFeO_{2.5}$ from polycrystalline synthesis (gray curve) superimposed with the frequencies of the calculated Raman active modes: blue bars represent A_g mode, red bar B_g modes (multiplied by a scaling factor 1.07).

Figure 1b show the spectra collected for $CaFeO_{2.5}$ sample either ground from the single crystal (black curve), so potentially textured, or from an independent polycrystalline synthesis (grey curve). In the powder grained from single crystal the texturing effect is not present (or not appreciable) and the two spectra are similar except for a different amount of background fluorescence. Due to the adopted scattering geometry, in such spectra the A_g modes should be preferentially selected and so we can assign the most intense frequencies at 705, 455, 381, 316, 290, 263, 253, and 188 cm^{-1} to the A_g symmetry. For the same reason, few less intense bands can be seen in spectra of Figure 1 and can be assigned to B_g modes.

We performed periodic DFT simulations of the $CaFeO_{2.5}$ structure to obtain the eigenfrequencies and polarizations for all Raman active vibrational modes. The frequencies are shown as bars in Figure 1b, with the blue one representing A_g modes and red ones all the other B_g modes. The comparison of calculated A_g mode frequencies with the experimental results is quite satisfactory, with frequencies below 500 cm^{-1} in accordance with a relative position error less than 3%. For higher frequency modes the absolute accordance is less accurate, probably due to the fact that PBE functional do not take in account the exact electron-electron exchange potential. Furthermore, the 3 A_g modes lying below 200 cm^{-1} cannot be experimentally detected due to the notch filter intensity suppression.

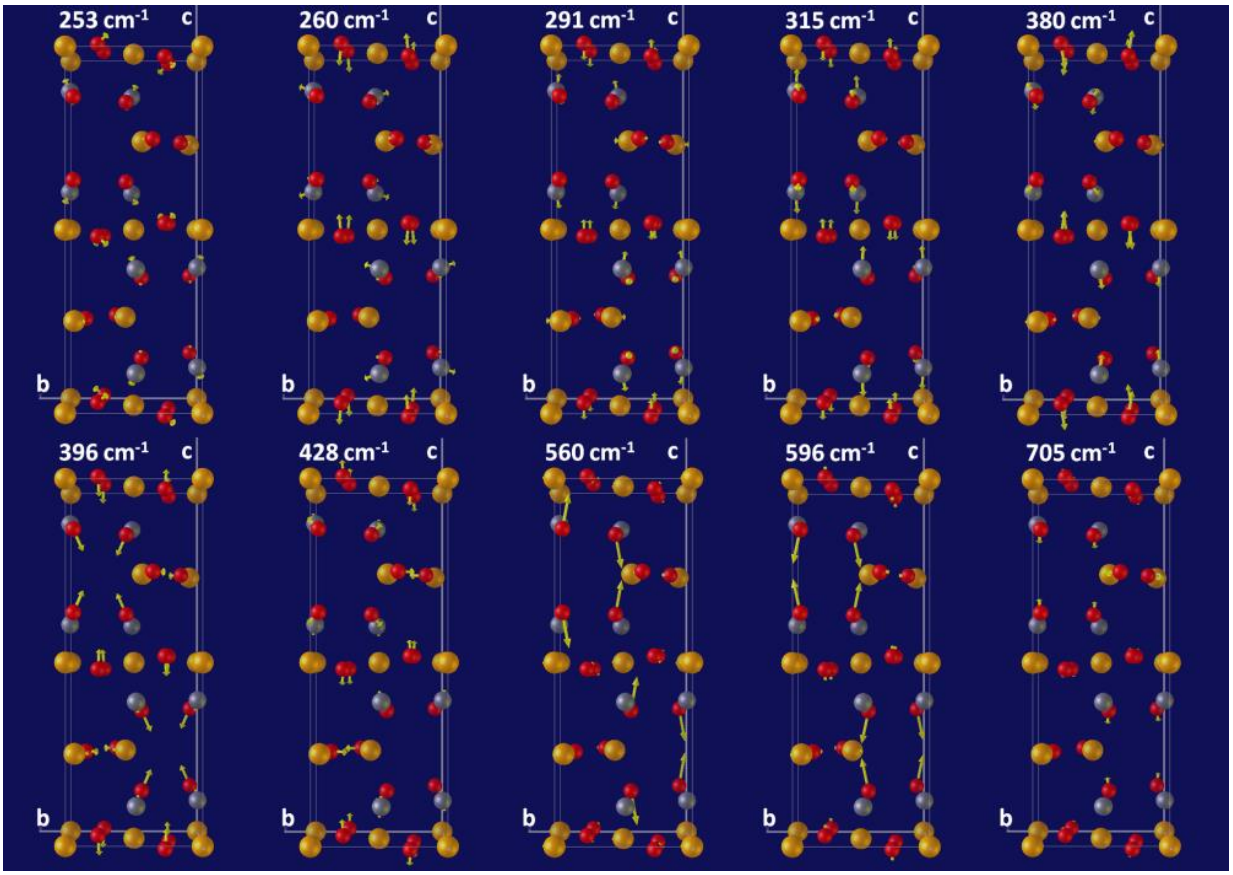

Figure 2: Computed polarizations for the Ag modes that have been detected in Raman scans. Many of these modes show a marked polarization of apical oxygen displacements along *b* direction.

From the comparison of calculations and the experimental results we were able to assign all of the A_g modes in the range 200-800 cm^{-1} and the respective calculated polarizations are shown in Figure 2. It is worth noticing that the majority of these modes show an enhanced displacement along the b-axis direction, in particular for the apical oxygen ions.

From DFT results it is also possible to gain a more detailed insight into the peculiar electronic arrangement that may explain the preference of $CaFeO_{2.5}$ for the *Pnma* space group compared to *I2mb*. While both structure models in *Pnma* and *I2mb* have been relaxed at a rather high level of precision, it was possible to bring to convergence both systems, which showed a comparable stability, being *Pnma* slightly more stable by only 0.02 eV (2.22 kJ/mol). Analyzing the electron density output for the *Pnma* case, shown in Figure 3a, it is clearly evident that the apical oxygen is more strongly bonded to the tetrahedral rather than the octahedral Fe atoms. This implies the presence of induced local dipoles along the *b*-axis direction. Unbalanced charge distribution is not observed in the *ac* planes cut at the octahedral plane (Figure 3b). At the tetrahedral (Figure 3c) layers, even if a symmetrical charge density is observed for all Fe-O bonds along each chain, the empty space in between them gives unbalanced charge distributions and with that induced dipole moments along c-axis direction. The strength of induced dipole interactions depends on the overlap of crystalline orbitals along the dipole moment direction. The anisotropic distribution

of electron clouds along the *b*-direction can develop to long range depending mainly on the orbitals overlap of Fe_{octa}–O_{ap} bonds (see Figure 3a). When this interaction exists it can be easily distorted by an external electric field, implying a high polarizability along that direction. In this way a perturbation along the *b* axis by the electric field of a laser is expected to produce intense Raman modes [42]. On the contrary, due to the scarce orbitals overlap in between two chains along c-direction, the polarizability should be weaker.

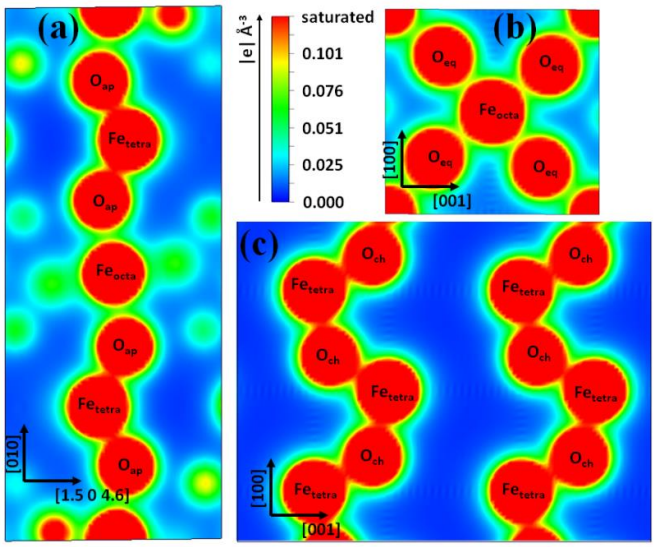

Figure 3. Electron density maps for the $CaFeO_{2.5}$ system in the *Pnma* space group: periodic DFT simulations with VASP code.[38] Octahedral and tetrahedral Fe atoms are labeled as Fe_{octa} and Fe_{tetra}, respectively, while O_{ap}, O_{eq}, and O_{ch}, refer to the oxygen atoms bridging Fe_{octa}-Fe_{tetra}, Fe_{octa}-$Fe_{octa,}$ and Fe_{tera}-Fe_{tetra}, respectively. Part (a): plane including O_{ap}, Fe_{octa} and Fe_{tetra} atoms, with the *b* axis vertical. Part (b) *ac* plane intercepting Fe_{octa}. Part (c) *ac* plane intercepting Fe_{tetra}. To allow a better resolution in the lower electron density region between adjacent atoms the color scale has been chosen in a way that it saturates in the proximity of the nuclei; in this way, Fe and O atoms have apparently the same electron density.

The results of the orientation dependent Raman experiments on $CaFeO_{2.5}$ single crystal are presented in Figure 4. Measurement with the ***E*** vector in the *a*,*b*, *b*,*c* and *a*,*c* planes are shown parts (a), (b) and (c), respectively. The most striking and interesting finding were obtained when the sample is rotated in such a way that ***E*** moves from parallel to perpendicular to the *b* axis, see parts (a) and (b). In such experiments the A_g modes at (705, 455, 381, 316, 290, 263, 253, and 188 cm^{-1}) are significantly enhanced when ***E*** // *b* and the enhancement progressively disappears when ***E*** moves towards the *a*- or *c*-axis. A final support of this picture is reported in Figure 4c, where the *b*-axis is out of the scattering plane, and no significant differences are observed along the crystal rotation.

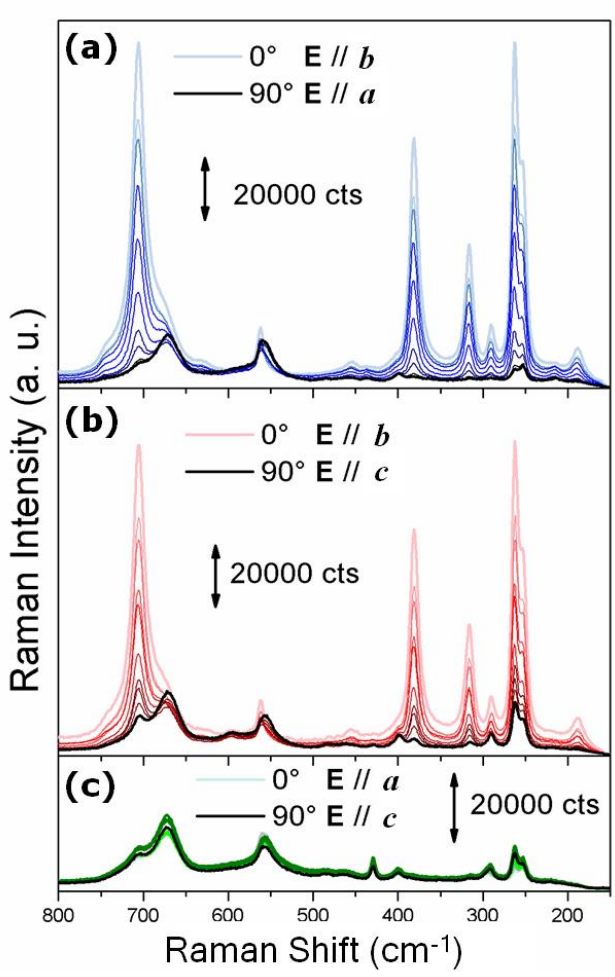

Figure 4. Raman spectra of $CaFeO_{2.5}$ single crystal for different orientations. From pale to black color, 9 spectra have been collected every 10 degrees of rotation in the scattering plane: Part (a) *a* and *b* axis in the scattering plane. Part (b): *b* and *c* axis in the scattering plane. Part (c): *a* and *c* axis in the scattering plane. The laser excitation light was λ = 785 nm. The spectra are collected in backscattering geometry with incoming light polarized along y. The scattered beam was integrated over all polarizations.

With the aim to correlate this striking orientation dependence of the Raman spectra of the $CaFeO_{2.5}$ system with the oxygen ordering properties of isomorphous brownmillerite systems, we compare Raman spectra of $SrFeO_{2.5}$ and $CaFeO_{2.5}$ powders (Figure 5 red vs. black or gray curves). In the Raman spectra collected on $CaFeO_{2.5}$ powders the A_g modes at (705, 455, 381, 316, 290, 263, 2.53, and 188 cm^{-1}) are still very strong, as a fraction of crystallites have the b-axis partially oriented along ***E***. The same random orientation of the *b*-axis holds for the $SrFeO_{2.5}$ powders too, that however does not show any strong Raman feature. Actually, the Raman spectrum of $SrFeO_{2.5}$ powders looks like the spectra of the $CaFeO_{2.5}$ system collected with ***E*** in the *ac* plane (Figure 4c). The structural changes obtained replacing Ca by Sr are mainly observed along the *b*-axis, where the Fe_{octa}-O_{ap} distances vary significantly from 2.12 Å to 2.20 Å, while both Fe_{oct}-O_{eq} and Fe_{tetra}-O_{ap} distances are much less affected by the A-cation nature.17,28. Moreover, as reported also by other authors, $SrFeO_{2.5}$ shows disorder on the *b* stacking direction.

The interlayer distance (along b-axis) of the interacting induced dipoles can be taken as the mid distance in between nearest Fe_{tetra}-O_{ap} in two successive layers, i. e. 5.7 Å for $CaFeO_{2.5}$ and 6.1 Å for $SrfeO_{2.5}$. The distance in between two chains that should correspond to the interaction range of intralayer (along *c*-axis) induced dipoles is 5.6 Å for $CaFeO_{2.5}$ and 5.7 Å for $SrFeO_{2.5}$.

The intralayer and interlayer interactions both participate in the ordering process as there is no advantage in compensating induced dipole interlayer or intralayer.

We showed that for $CaFeO_{2.5}$ the interlayers interactions are present (see Figure 4) and, from the similarity of the distance with intralayer interaction, we can affirm that the two are in competition and create a three dimensional ordered structure. On the contrary we showed that for $SrFeO_{2.5}$ the interlayers interactions are suppressed, or by far reduced, (see Figure 5a) and this goes along with the disporoportional increase of the interlayer interaction distance respect to the intralayer one. As consequence the decreased orbital overlap of Fe_{octa}-O_{ap} decreases the interaction strength and correlation length and becomes more advantageous compensating the dipoles only intralayers.

The Raman spectra reported in Figure 5b have been collected under resonant Raman conditions (see Figure 1a) and in particular the 442 nm line excites orbitals participating to the total-symmetric stretching mode at 700 cm^{-1}. Indeed in the spectrum of $CaFeO_{2.5}$ this mode is by far the most intense appreciable under resonant conditions. This means that its relative intensity with respect to the other adjacent modes has been increased by some order of magnitude due to resonant condition. For the $SrFeO_{2.5}$ framework total-symmetric stretching mode should be similar to $CaFeO_{2.5}$ and then resonance condition would apply the same. In the red spectrum of Figure 5b the mode at 662 cm^{-1} is the one which results to be by far the most enhanced and then we assigned it to octahedron unit of $SrFeO_{2.5}$. These results highlight that in both samples the alternating octahedra plus tetrahedral blocks (as specific units of the structure) are present and that the consistent shift in frequency of the vibration suggest a different bond force constant.

In the non-resonant case (see Figure 5a), the breathing mode of octahedra is almost one order of magnitude less intense for the $SrFeO_{2.5}$ system than in $CaFeO_{2.5}$, while their relative intensity is comparable in the resonant case (see Figure 5b). This can be explained by the fact that resonant Raman excites vibrational modes of the same local unit engaged in the electronic transition and exhibiting the same symmetry [35, 36, 43-45], while first order Raman analyze the spatial coherence of all the units vibrating together. Moreover, the FWHM obtained by fitting the mode in non-resonant condition with a Lorentzian distribution give 19.6 cm^{-1} for $CaFeO_{2.5}$ while 26.8 cm^{-1} for $SrFeO_{2.5}$, pointing out a certain degree of damping in the latter system connected to a shorter range of coherence of this lattice vibration.

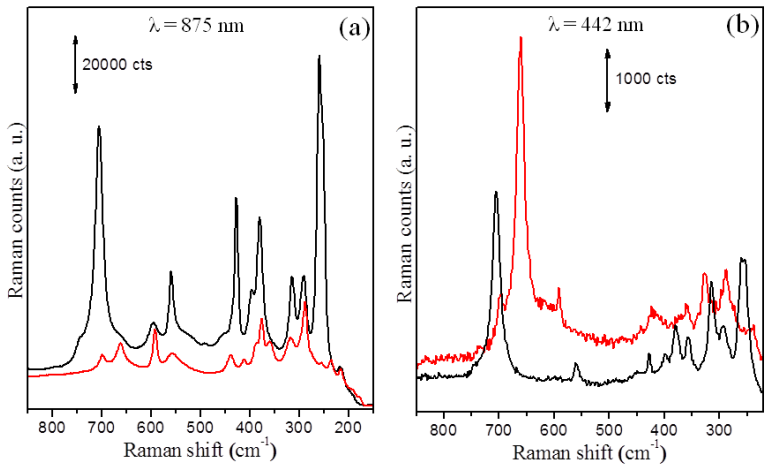

Figure 5: Raman spectra of CaFeO2.5 (black line) and SrFeO2.5 powder (red line). For the SrFeO25 system only polycrystalline samples are available. (a) Scans with laser excitation light at λ = 785 nm. (b) Scans in resonance mode with laser excitation light at λ = 442 nm. Note how the totalsymmetric stretching on $SrFeO_{2.5}$ is almost suppressed in normal Raman, while well visible when resonantly excited.

The same mode appears red shifted by $\Delta\omega$ = 43 cm^{-1} in the case of $SrFeO_{2.5}$. For a total-symmetric A_g stretching mode, the frequency (ω) can be directly related to the equilibrium Fe_{octa}-O bond distance through the force constant (k) and the reduced mass (μ) of the oscillator ($\omega = \sqrt{(k/\mu)}$ in the harmonic approximation). Considering a single Fe_{octa}-O vibration (where μ is the same in both systems), calculation of force constant gives a value of 366 N/m for the Ca containing material and 322 N/m for the Sr one. This corresponds to a decrease in the restoring force of about 10% for the latter system. As far as axes *a* and *c* do not vary considerably for the two systems and so the Fe_{octa}-O_{eq} bonds, that indeed is 1.967 Å for $CaFeO_{2.5}$ and 1.985 Å for $SrFeO_{2.5}$. This decrease of restoring force is directly related to the difference in the Fe_{octa}-O_{ap} bond (2.11 Å for $CaFeO_{2.5}$ and 2.20 Å for $SrFeO_{2.5}$). All these finding together are in agreement with a picture where O_{ap} in $SrFeO_{2.5}$ is weakly bonded to the octahedron unit and may more easily separate from it. The situation comes dramatic when passing to the $SrFeO_{2.5}$ systems that can be then better modeled as a succession of tetrahedra and square planar layers where interlayer interactions are weakened or totally hindered by the reduced overlap of orbitals of apical oxygen with the square plane ones.

Analogously, the rocking mode at 263 cm^{-1} for the $CaFeO_{2.5}$ system (see Figure 4a) should be slightly red-shifted for the $SrFeO_{2.5}$ material too. Anyhow a $\Delta\omega$ value smaller than 43 cm^{-1} is expected as the Fe_{tera}-O_{ap} bond length much more similar in the two systems (1.862 Å for $CaFeO_{2.5}$ and 1.848 Å for $SrFeO_{2.5}$). Indeed a band at 235 cm^{-1} is observed in the $SrFeO_{2.5}$ spectrum reported in Figure 4a. The low intensity of such mode, with respect to the sharp and intensy reported for $CaFeO_{2.5}$, point out the more localized nature of the crystal orbitals involved that produce less intense induced dipoles that, in turn give less intense Raman bands.

Conclusions

Our simulations showed that there is a net dipole formed in between Fe_{octa}-Fe_{tetra} in the different layer coming from a non balanced charge due to the different covalency and bond distance of Fe_{tetra}-O_{ap} and Fe_{octa}-O_{ap} bonds. From the orientation dependent measurements here presented we showed that the effect is present in the highly ordered $CaFeO_{2.5}$ system as intense bands emerge when electric field of laser is parallel to *b* axis.

Indeed, if there is a dipole-dipole interaction in between two layers, we expect a laser line can perturb it due to strong anisotropy of charge distribution and relatively long range of this interaction. In this case, when laser line is parallel to the direction of this interaction, i. e. *b* direction in our case, we expect large polarizabilites and consequent high Raman intensities for the modes connected to this interaction. The relatively short *b*-axis (14.77 Å) of the $CaFeO_{2.5}$ system,[27] makes the interlayer dipole-dipole interaction effective, forcing the structure to belong to the *Pnma* space group. On the contrary if the dipole-dipole interaction is not present, or weak, we expect that long range interlayer organization of charges is not present and consequently the polarizability coming from deformation of more localized charges should be highly damped and so intensities. We showed, by first-order Raman and resonant Raman techniques, that this is the case for $SrFeO_{2.5}$ system. The longer *b*-axis of the $SrFeO_{2.5}$ system (15.57 Å) [15] weaken the interaction among Fe_{octa}–O_{ap}, and consequently less interacting dipoles, making energetically almost equivalent any orientation of the tetrahedra between different layer. No particular disordering fingerprint have been found for the *a* and *c* directions.

It is worth noticing that the loss of interlayer ordering (i.e. loss of ordering in the *b* direction) is associated, for the mixed valence Brownmillerite materials, with an anomalous displacement of O_{ap} species. The observed formation of extended phase boundaries in these materials starting from an ordered structure can be accomplished only with a collective motion of these oxygen species. A single hopping mechanism requires a too high energy barrier to be possible at moderate temperatures and will certainly destroy chain ordering within *ac* plane, fact that has not been found. On the contrary the scheme well adapt to the two step collective mechanism of oxygen mobility ($O_{ap} \rightarrow O_{eq'}$ and $O_{eq''} \rightarrow O_{ap}$) presented by Paulus et al. [16]. Indeed, if from one side it is able to explain the formation of interlayer disorder while intralayer order is maintained, the same mechanism is at the basis of the know oxygen ionic conduction of SFO at low temperature. Nevertheless the relevant modes for diffusion are located at low frequency and this aspect can be better analyzed by neutron spectroscopy and will be the core of a subsequent publication.

Acknowledgements

We are grateful to A. Damin (University of Turin, I) for the help in Raman laboratory.

Corresponding Author

*E-mail: piovano@ill.fr

Notes

The authors declare no competing financial interest.

Referencees

[1] Mamak M, Coombs N and Ozin G 2000 *Journal of the American Chemical Society* **122** 8932
[2] Dusastre V and Kilner J A 1999 *Solid State Ionics* **126** 163
[3] Goodenough J B 2003 *Annual Review of Materials Research* **33** 91
[4] Ormerod R M 2003 *Chemical Society Reviews* **32** 17
[5] Zhu W Z and Deevi S C 2003 *Materials Science and Engineering a-Structural Materials Properties Microstructure and Processing* **362** 228
[6] Mamak M, Metraux G S, Petrov S, Coombs N, Ozin G A and Green M A 2003 *Journal of the American Chemical Society* **125** 5161
[7] Adler S B 2004 *Chemical Reviews* **104** 4791
[8] Zuo C, Zha S, Liu M, Hatano M and Uchiyama M 2006 *Advanced Materials* **18** 3318
[9] Tsipis E V and Kharton V V 2008 *Journal of Solid State Electrochemistry* **12** 1367
[10] Brett D J L, Atkinson A, Brandon N P and Skinner S J 2008 *Chemical Society Reviews* **37** 1568
[11] Jacobson A J 2010 *Chemistry of Materials* **22** 660
[12] Cai Z H, Kuru Y, Han J W, Chen Y and Yildiz B 2011 *Journal of the American Chemical Society* **133** 17696
[13] Shin T H, Ida S and Ishihara T 2011 *Journal of the American Chemical Society* **133** 19399
[14] Munoz-Garcia A B, Bugaris D E, Pavone M, Hodges J P, Huq A, Chen F L, zur Loye H C and Carter E A 2012 *Journal of the American Chemical Society* **134** 6826
[15] Le Toquin R, Paulus W, Cousson A, Prestipino C and Lamberti C 2006 *Journal of the American Chemical Society* **128** 13161
[16] Paulus W, Schober H, Eibl S, Johnson M, Berthier T, Hernandez O, Ceretti M, Plazanet M, Conder K and Lamberti C 2008 *Journal of the American Chemical Society* **130** 16080
[17] Piovano A, Agostini G, Frenkel A I, Bertier T, Prestipino C, Ceretti M, Paulus W and Lamberti C 2011 *Journal of Physical Chemistry C* **115** 1311
[18] Abakumov A M, Alekseeva A M, Rozova M G, Antipov E V, Lebedev O I and Van Tendeloo G 2003 *Journal of Solid State Chemistry* **174** 319
[19] Abakumov A M, Kalyuzhnaya A S, Rozova M G, Antipov E V, Hadermann J and Van Tendeloo G 2005 *Solid State Sciences* **7** 801
[20] D'Hondt H, Abakumov A M, Hadermann J, Kalyuzhnaya A S, Rozova M G, Antipov E V and Van Tendeloo G 2008 *Chemistry of Materials* **20** 7188
[21] Krekels T, Milat O, Vantendeloo G, Amelinckx S, Babu T G N, Wright A J and Greaves C 1993 *Journal of Solid State Chemistry* **105** 313
[22] Lambert S, Leligny H, Grebille D, Pelloquin D and Raveau B 2002 *Chemistry of Materials* **14** 1818
[23] Hadermann J, Abakumov A M, D'Hondt H, Kalyuzhnaya A S, Rozova M G, Markina M M, Mikheev M G, Tristan N, Klingeler R, Buchner B and Antipov E V 2007 *Journal of Materials Chemistry* **17** 692
[24] Kruger H and Kahlenberg V 2005 *Acta Crystallographica Section B-Structural Science* **61** 656
[25] Kruger H, Kahlenberg V, Petricek V, Phillipp F and Wertl W 2009 *Journal of Solid State Chemistry* **182** 1515

[26] Lazic B, Kruger H, Kahlenberg V, Konzett J and Kaindl R 2008 *Acta Crystallographica Section B-Structural Science* **64** 417
[27] Ceretti M, Piovano A, Cousson A, Berthier T, Meven M, Agostini G, Schefer J, Hernandez O, Lamberti C and Paulus W 2012 *CrystEngComm* **14** 5771
[28] Auckett J E, Studer A J, Pellegrini E, Ollivier J, Johnson M R, Schober H, Miiller W and Ling C D 2013 *Chemistry of Materials* **25** 3080
[29] Munoz A, de la Calle C, Alonso J A, Botta P M, Pardo V, Baldomir D and Rivas J 2008 *Physical Review B* **78**
[30] Zainullina V M, Leonidov I A and Kozhevnikov V L 2002 *Physics of the Solid State* **44** 2063
[31] Stolen S, Bakken E and Mohn C E 2006 *Physical Chemistry Chemical Physics* **8** 429
[32] Mohn C E, Allan N L, Freeman C L, Ravindran P and Stolen S 2004 *Physical Chemistry Chemical Physics* **6** 3052
[33] Shein I R, Kozhevnikov V L and Ivanovskii A L 2006 *Journal of Physics and Chemistry of Solids* **67** 1436
[34] Lontsi-Fomena M, Villesuzanne A, Doumerc J P, Frayret C and Pouchard M 2008 *Computational Materials Science* **44** 53
[35] Ricchiardi G, Damin A, Bordiga S, Lamberti C, Spanò G, Rivetti F and Zecchina A 2001 *J. Am. Chem. Soc.* **123** 11409
[36] Bordiga S, Damin A, Bonino F, Ricchiardi G, Zecchina A, Tagliapietra R and Lamberti C 2003 *Phys. Chem. Chem. Phys.* **5** 4390
[37] Eilertsen E A, Giordanino F, Lamberti C, Bordiga S, Damin A, Bonino F, Olsbye U and Lillerud K P 2011 *Chemical Communications* **47** 11867
[38] Kresse G and Furthmuller J 1996 *Physical Review B* **54** 11169
[39] Tobbens D M and Kahlenberg V *Vibrational Spectroscopy* **56** 265
[40] Merrick J P, Moran D and Radom L 2007 *Journal of Physical Chemistry A* **111** 11683
[41] Aroyo M I, Kirov A, Capillas C, Perez-Mato J M and Wondratschek H 2006 *Acta Crystallographica Section A* **62** 115
[42] Wolverson D in *Characterization of Semiconductor Heterostructures and Nanostructures II* (Eds.: C. Lamberti, G. Agostini), Elsevier, Amsterdam, **2013**, pp. 753
[43] Damin A, Bonino F, Bordiga S, Groppo E, Lamberti C and Zecchina A 2006 *Chemphyschem* **7** 342
[44] Vishnuvarthan M, Paterson A J, Raja R, Piovano A, Bonino F, Gianotti E and Berlier G 2011 *Microporous and Mesoporous Materials* **138** 167
[45] Bonino F, Damin A, Piovano A, Lamberti C, Bordiga S and Zecchina A 2011 *Chemcatchem* **3** 139